

Original Article

# Neuroimaging Assessment of the Therapeutic Mechanism of Acupuncture and Bee Venom Acupuncture in Patients with Idiopathic Parkinson's Disease: A Double-blind Randomized Controlled Trial

Young-Eun Lee<sup>1,2†</sup>, Seung-Yeon Cho<sup>2†</sup>, Han-Gyul Lee<sup>3</sup>, Seungwon Kwon<sup>3</sup>, Woo-Sang Jung<sup>3</sup>, Sang-Kwan Moon<sup>3</sup>, Jung-Mi Park<sup>2</sup>, Chang-Nam Ko<sup>2</sup>, Seong-Uk Park<sup>2\*</sup>

<sup>1</sup>Department of Clinical Korean Medicine, Graduate School, Kyung Hee University, Seoul, Republic of Korea

<sup>2</sup>Stroke and Neurological Disorders Center, Kyung Hee University College of Korean Medicine, Kyung Hee University Hospital at Gangdong, Seoul, Republic of Korea

<sup>3</sup>Department of Cardiology and Neurology, Kyung Hee University College of Korean Medicine, Kyung Hee University Medical Center, Seoul, Republic of Korea

**Objectives:** The purpose of this study was to explore the therapeutic mechanism of acupuncture and bee venom acupuncture (BVA) in patients with idiopathic Parkinson's disease (IPD) using positron emission tomography (PET) and arterial spin labeling (ASL).

**Methods:** Patients with IPD who received a stable dose of anti-parkinsonian medication for at least 4 weeks were recruited and randomly divided into one of two groups: treatment and control. The treatment group (11 subjects) received acupuncture and BVA at acupoints, and the control group (9 subjects) received sham acupuncture and normal saline injections at non-acupoints, twice per week for 12 weeks. The patients were examined using PET and ASL at baseline and after the 12-week treatment. In addition, age- and sex-matched healthy subjects without neurological symptoms and history were recruited to compare ASL data of patients with IPD.

**Results:** PET results revealed that striatal dopamine transporter binding increased in each group after 12 weeks. Although the change was larger in the treatment group, the difference was not statistically significant. In ASL results, the treatment group exhibited hyperperfusion in specific regions compared with the healthy control group. After 12 weeks' intervention, hyperperfusion regions were recovered only in the treatment group. In contrast, significant changes were not found in hyperperfusion regions in the control group after 12 weeks.

**Conclusions:** Our findings suggest that the therapeutic mechanisms of acupuncture and BVA in IPD are different from placebo and operate by altering dopamine availability and recovering hyperactivity in cerebral blood flow.

**Key Words** : acupuncture; bee venom acupuncture; Parkinson's disease; neuroimaging; PET; ASL

## Introduction

Parkinson's disease (PD) is the second most

common neurodegenerative disorder. The four main symptoms of PD are resting tremor, bradykinesia, rigidity, and postural instability. The

• Received : 20 October 2023      • Revised : 13 November 2023      • Accepted : 15 November 2023

• Correspondence to : Seong-Uk Park

Stroke and Neurological Disorders Center, Kyung Hee University Hospital at Gangdong,  
892 Dongnam-ro, Gangdong-gu, Seoul, 05278, Republic of Korea.

Tel : +82-2-440-6217, FAX : +82-2-440-7171, E-mail : seonguk.kr@gmail.com

† These authors contributed equally to this work.

pathophysiological mechanisms of PD remain unclear; however, deficits in dopaminergic nigrostriatal neurons in the substantia nigra pars compacta have been implicated.<sup>1)</sup>

Acupuncture has been used to relieve PD-like symptoms in Asian countries for centuries. Many studies have described the neuroprotective and anti-neuroinflammatory effects of acupuncture and bee venom acupuncture (BVA) for treating PD.<sup>2-4)</sup> In the previous clinical trials that we conducted,<sup>5,6)</sup> acupuncture and BVA also demonstrated promising results as adjunctive therapies for patients with idiopathic PD (IPD).

However, the therapeutic mechanism of acupuncture and BVA in PD remains uncertain, and several studies are ongoing. Kim et al.<sup>7)</sup> found that acupuncture treatment at GB34 in 1-methyl-4-phenyl-1,2,3,6-tetrahydropyridine (MPTP)-intoxicated mice appeared to improve motor function through an increase in dopamine availability in the synaptic cleft, likely through enhanced dopamine release, which may result in the normalization of postsynaptic abnormalities. Some clinical studies have been conducted to identify the therapeutic mechanism of acupuncture in PD using functional magnetic resonance imaging (fMRI).<sup>8,9)</sup> In these studies, neural responses after acupuncture at GB34 of patients with PD were compared with those of healthy subjects.

With technical advances in neuroimaging, positron emission tomography (PET) has been used for differential diagnosis and understanding of the pathophysiology of PD, and is considered to be an excellent tool to evaluate complications in PD and ongoing management.<sup>10)</sup> In addition,

arterial spin labeling (ASL) is also used for diagnosis, monitoring disease progression, and evaluation of treatment effect in patients with PD.<sup>11)</sup> The density of striatal dopamine transporter (DAT) can be measured using PET and ASL, which are used to examine regional metabolism and neural activity through measuring changes in regional cerebral blood flow (CBF), and are known to be suitable for studying relatively long-term effects on CBF both at rest and during activation.<sup>12-14)</sup>

In the present randomized-controlled, double-blind clinical trial, we performed acupuncture and BVA treatment in patients with IPD, and attempted to explore therapeutic mechanisms by observing DAT and CBF using PET and ASL.

## Methods

### 1. Ethics statement

The study was performed in accordance with ethics standards of the Helsinki Declaration. The protocol was approved by the Institutional Review Board of the Kyung Hee University Hospital at Gangdong (KHNMC-OH-IRB-2012 01-013). After full description of the study, written informed consent was obtained from all subjects.

### 2. Participants

This study was conducted between November 2012 and September 2014 at Kyung Hee University Hospital at Gangdong, Korea. Subjects were recruited through the hospital's website and bulletin boards. Interested subjects contacted the study coordinator for further information. Potential

subjects were then offered a formal in-person assessment. The inclusion criteria were as follows: diagnosis of IPD according to the United Kingdom Parkinson's Disease Society Brain Bank criteria;<sup>15)</sup> administration of a stable dose of anti-parkinsonian medication for at least 4 weeks before the study; patients in Hoehn and Yahr stage 1-4;<sup>16)</sup> a score > 1 in  $\geq 2$  categories of the Unified Parkinson's Disease Rating Scale (UPDRS) part III, including tremor, rigidity, bradykinesia, and postural instability; and a Mini-Mental State Examination-Korean version (MMSE-K) score > 24. Exclusion criteria were as follows: (presence of) epilepsy, dementia, alcohol or drug addiction, or a history of having received psychiatric medication; secondary Parkinsonism caused by cerebrovascular disease, neoplasm, or infection; Parkinson-plus syndromes; pregnancy; or a positive response to a bee venom skin allergy test. The drop out criteria included: not undergoing > 8 of a total of 24 treatment sessions; serious adverse events; or withdrawal of agreement to participate in the study.

In addition, age- and sex-matched healthy subjects without neurological symptoms and history were recruited to compare ASL data of patients with IPD.

### 3. Study Design

This study was a randomized-controlled, double-blind clinical trial. The patients were surveyed regarding sex, age, medical history, duration of disease and medications, and evaluated using the MMSE-K. After the patients were randomized into a treatment or control (sham treatment) group in a ratio of 1:1 using a

sealed envelope method by a researcher not involved in the assessments and interventions, a skin test was performed to confirm whether subjects were allergic to bee venom. Bee venom diluted to 0.005% in normal saline was used for the treatment group. A 0.1 mL injection was performed at the unilateral LI11 (*Quchi*) acupuncture point using an insulin syringe (BD Ultra-Fine II, Becton, Dickinson Company, USA). Development of a wheal > 5 mm in diameter, a rash > 10 mm in diameter, or severe itching at the site within 15-20 min was considered to indicate bee venom allergy and, accordingly, the subject was excluded from the study. For blinding, the skin test was performed using the same method and normal saline in the control group. Thereafter, the subjects underwent baseline assessments including PET and ASL. From the second visit after the baseline assessments, the treatment group received acupuncture and BVA treatments at acupuncture points, while the control group received sham acupuncture and normal saline injection at non-acupoints, twice per week for 12 weeks. After 12 weeks of interventions, all subjects underwent PET and ASL again, and the study was completed. In addition, healthy subjects underwent ASL once at baseline. All assessments and statistical analyses were completed by researchers who were masked to the allocation.

### 4. Interventions

All interventions were performed by a single Korean Medicine doctor with more than 10 years' experience. The treatment group received acupuncture and BVA treatments at 10

acupuncture points: bilateral GB20 (*Fengchi*), LI11 (*Quchi*), GB34 (*Yanglingquan*), ST36 (*Zusanli*), and LR3 (*Taichong*). Bee venom (0.1 mL) diluted to 0.005% in normal saline (Yumil Farm, Korea) was injected into each point, and then sterile, disposable, stainless steel acupuncture needles (diameter = 0.25 mm, length = 30 mm, Dongbang, Korea) were inserted into the points listed above to a depth of 0.5 - 1.0 cm and rotated at 2 Hz for 10 s to achieve *deqi*, the sensation felt by the subject when the acupuncture needle is in the adequate position for clinical efficacy. This needle position was maintained for 15 min. The concentration and dose of bee venom and acupuncture points were determined based on our pilot study.<sup>5)</sup> The control group received sham treatments. Normal saline (0.1 mL) was injected into 10 non-acupuncture points: bilateral inferior from GB20 (*Fengchi*) 5 cm, lateral from LI10 (*Shousanli*) 2 cm, inferior from GB34 (*Yanglingquan*) 5 cm, posterior from SP9 (*Yinglingquan*) 2 cm, and superior from LR2 (*Xingjian*) 1 cm. Subsequently, shallow, minimal acupuncture stimulation was performed at the same points using the same acupuncture needle for 15 min without *deqi*. The healthy control group did not receive any treatments.

## 5. PET/Computed Tomography

F-18 fluoropropylcarbomethoxyiodophenyl-nortropane (FP-CIT) PET/computed tomography (CT) was performed using a Philips Gemini Time-of-Flight (TOF) PET/CT instrument (Philips Medical System, Netherlands). Antiparkinsonian drugs were discontinued 12 h before the scans were performed. Image acquisition was started 3

h after intravenous injection of F-18 FP-CIT (185 MBq). Emission PET data were acquired for 10 min in the three-dimensional (3D) mode after brain CT, which was performed in the spiral mode at 120 kVp and 50 mA. PET images were reconstructed using TOF-ordered subset expectation maximization. PET imaging was automatically obtained in an area over 40% of the maximum value around the left and right striatum of the patient using 3D region of interest (ROI) software (Philips Medical Systems, Netherlands).<sup>17)</sup> Changes over a 12-week period in the small intake side from the results of the primary PET data were evaluated.

## 6. Magnetic Resonance Imaging

All magnetic resonance (MR) images were acquired using a 3.0 Tesla scanner (Philips Medical Systems, Netherlands) equipped with an 8-channel phase-array coil. For pulsed ASL (PASL) data, echo-planar MR imaging and signal targeting with alternative radiofrequency (EPSTAR) method<sup>18)</sup> was used for labeling arterial blood, and single-shot echo planar imaging (EPI) sequence was used for imaging acquisition.<sup>19)</sup> The following parameters were used: fast field echo (FFE), repetition time (TR) / echo time (TE) = 3,000 / 6.1 ms; flip angle = 90°; sensitivity encoding (SENSE) factor = 2.3; 60 pairs of labeled-control, field of view (FOV) = 220 × 220 mm<sup>2</sup>, 15 slices; matrix size = 64 × 55; acquisition voxel size = 3.44 × 3.95 × 5.5 mm<sup>3</sup>; reconstructed voxel size = 1.96 × 1.96 × 5.5 mm<sup>3</sup>; label thickness = 130 mm; and slice thickness/gap = 5.5 / 1.2 mm. The time interval between the center of the labeling pulse and the starting point

of the periodic saturation pulse (TI1) was 700 ms. The time interval between the center of the labeling pulse and the center of the excitation pulse in EPI acquisition (TI2) was 1800 ms.

In addition, for using partial volume correction (PVC) and image registration of PASL data to a brain anatomy template, isotropic sagittal structural volumetric 3D-T1 weighted images were acquired using a magnetization-prepared rapid acquisition of gradient echo (MPRAGE) sequence.<sup>20)</sup> The following parameters were used: FFE, TR/TE, 8.1/3.7 ms; flip angle, 8°; FOV, 236 × 236 mm<sup>2</sup>, 187 slices; matrix size, 236 × 236; acquisition voxel size = 1 × 1 × 1 mm<sup>3</sup>; and reconstructed voxel size, 0.92 × 0.92 × 1 mm<sup>3</sup>.

## 7. Pre-processing of MR imaging data

Pre-processing of all MR imaging data was performed using Statistical Parametric Mapping (SPM) 8 software (Wellcome Department of Neurology, University College London, UK) in Matlab 6.5 (Mathworks, Inc, USA). The acquired raw data were converted from Philips format to analyze format using MRIcro (version 1.40, Neuropsychology Lab, Columbia SC, USA). To minimize the effect of subject movement in MR imaging, mean CBF maps were generated after the realignment of ASL images using SPM. For the PASL MRI data, EPI of each subject was realigned to the first volume and resliced according to any motion. The voxel-based CBF for each subject was then mapped using an ASL data processing toolbox (ASLtbx).<sup>21)</sup> Then, mean CBF maps were co-registered in 3D-T1 weighted image. 3D-T1 weighted images were segmented and entered in DARTEL, a diffeomorphic image

registration toolbox algorithm to create templates.

<sup>22)</sup> CBF values were corrected (CBFcorrect) to minimize partial volume effect and increase statistical power using the formula:  $CBF_{correct} = CBF_{uncorrect} / [\text{gray matter (GM)} + 0.4 \times \text{white matter (WM)}]$ .<sup>20)</sup> Finally, normalized CBF maps were smoothed with full-width of half maximum (FWHM) of 10 × 10 × 12.

## 8. Statistical analysis

Statistical analysis of ASL data was performed using SPM 8 software (Matlab 6.5). To confirm changes in specific brain regions, MNI coordinates were converted to Talairach coordinates using GingerALE and Talairach Client (University of Texas Health Science Center San Antonio, UTHSCSA). ASL data were analyzed using whole-brain voxel-based analysis for qualitative assessment. Comparison between the patient and healthy subjects was performed using the two-sample t-test, with sex and age as covariates, at a voxel level significance threshold of  $p < 0.05$  corrected for Family-wise error (FWE) rate with a cluster size  $\geq 20$  voxels. Comparison between before and after treatment in the treatment and control groups was performed using paired t-test at a voxel level with a significance threshold of  $p < 0.001$  corrected for false discovery rate (FDR) with a cluster size  $\geq 20$  voxels.

SPSS version 18.0 (IBM Corporation, Armonk, NY, USA) for Windows (Microsoft Corporation, Redmond, WA, USA) was used for statistical analysis of other data;  $p < 0.05$  was considered to be statistically significant. The baseline characteristics of patients with IPD were analyzed using the Mann-Whitney test for continuous variables, and

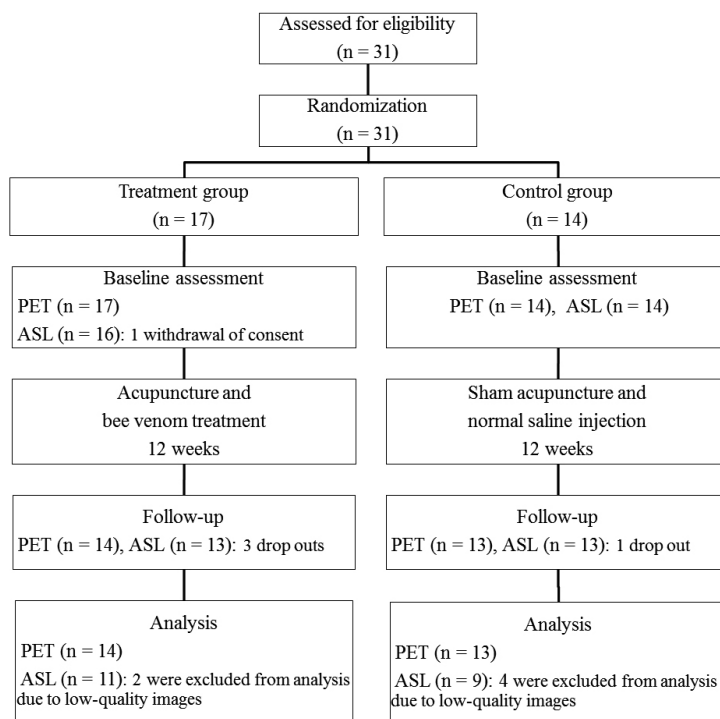


Fig. 1. Participant flow

PET: positron emission tomography, ASL: arterial spin labeling

chi-squared test and Fisher’s exact test for categorical variables. Comparison between the treatment and control groups was performed using the Mann-Whitney test for intergroup comparison, and Wilcoxon signed rank test for in-group comparison.

## Results

### 1. Participants

A total of 31 patients with IPD were randomly assigned to either the treatment group (n = 17) or control group (n = 14); participant flow is summarized in Figure 1. A total of 16 healthy subjects were age- and sex-matched with patients

with IPD. In the healthy control group, one subject dropped out after ASL was performed because of abnormal neuroimaging results, and another was excluded from the analysis due to low-quality images. Therefore, data from 14 healthy subjects were analyzed. No significant difference in age or sex was found between the patient and healthy groups. Between the treatment and the control groups, there was no significant difference in age, sex, duration of disease, Hoehn and Yahr stage, and UPDRS scores at baseline (Table 1).

### 2. DAT binding with F-18 FP-CIT PET

The PET data of the treatment group (n = 14)

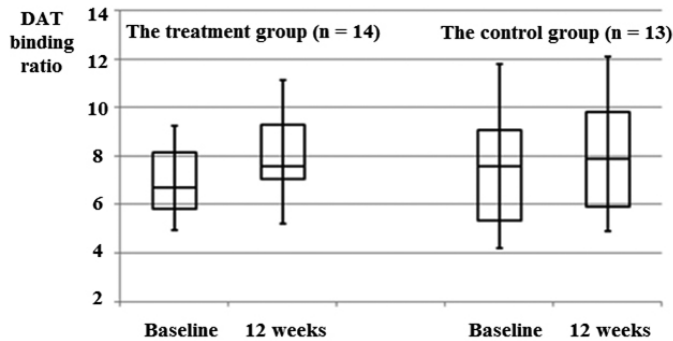


**Fig. 2.** Changes in striatal dopamine transporter (DAT) binding between the treatment and the control groups. Striatal DAT binding was increased 9.86% in the treatment group and 6.58% in the control group after 12 weeks; however, there was no statistically significant difference ( $p = 0.084$ ,  $p = 0.382$ , respectively).

and the control group ( $n = 13$ ) were analyzed. DAT binding in the striatum was increased after 12 weeks in both groups (treatment group, 9.86%; control group, 6.58%); however, there was no statistically significant difference ( $p = 0.084$ ,  $p = 0.382$ , respectively) (Figure 2).

### 3. Comparison of CBF measured using ASL between patients with IPD and the healthy group

Whole-brain voxel-based analysis of CBF images was performed in 14 age-matched healthy subjects and 20 patients with IPD. The patient group exhibited increased CBF (hyperperfusion) compared with the healthy group. Although there were hypoperfusion regions in the patient group compared with the healthy group, these were insignificant because of location, and considered to be artifacts (Figure 3). Hyperperfusion regions in the patient group included the bilateral insula,

**Table 1.** Baseline Characteristics of Patients with Idiopathic Parkinson’s Disease

	PET group			ASL group		
	Treatment group (n = 14)	Control group (n = 13)	<i>p</i> -value	Treatment group (n = 11)	Control group (n = 9)	<i>p</i> -value
Age (yr)	66.5 (58, 68.25)	61 (50, 65.5)	0.105	67 (58, 69)	64 (50, 66.5)	0.201
Male / Female	8 / 6	6 / 7	0.568	6 / 5	3 / 6	0.406
Duration of disease (mo)	42 (21, 99)	72 (24, 102)	0.488	24 (24, 60)	72 (12, 102)	0.656
Hoehn-Yahr stage	1.75 (1, 2.125)	2.5 (1, 3)	0.519	2 (1.5, 2.5)	2.5 (1, 3)	0.882
UPDRS subscore	Part II	12 (8, 15.5)	0.105	12 (8, 17)	17 (12, 22)	0.067
	Part III	15 (10, 16.25)	0.068	15 (10, 17)	18 (13, 23.5)	0.131
	Part II + III	26.5 (18.5, 32.25)	0.105	27 (19, 33)	30 (26.5, 46)	0.095

Values are median (lower quartile, upper quartile) or number. PET: positron emission tomography, ASL: arterial spin labeling. UPDRS: Unified Parkinson’s disease Rating Scale; UPDRS part II: Activities of daily living; UPDRS part III: Motor examination  $P < 0.05$ , statistically significant

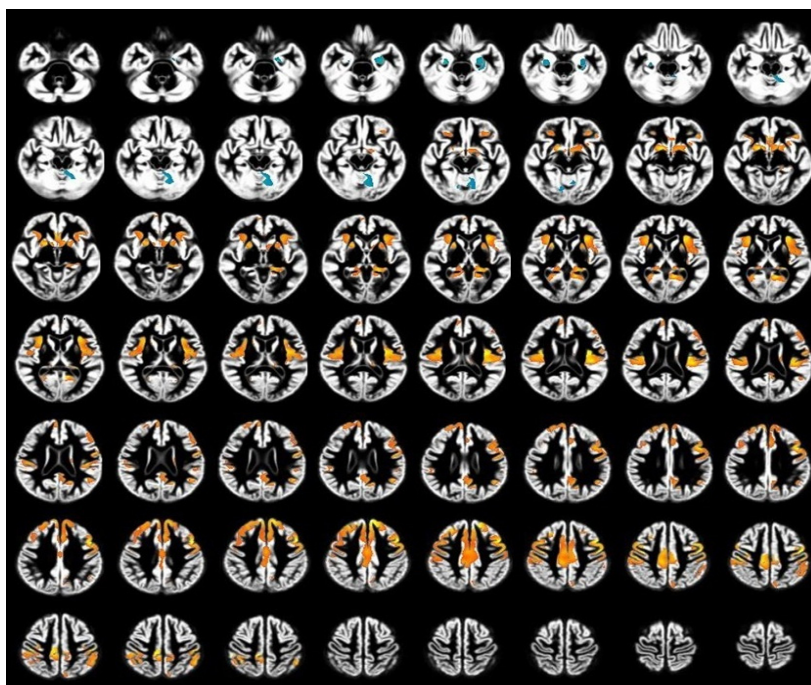


**Fig. 3.** Overlay of results of voxel-wise comparison between the patient and healthy groups

Overlaid images show hyperperfusion regions (red color) and hypoperfusion regions (blue color) of the patient group compared with those of the healthy group. These hypoperfusion regions were considered to be artifacts.

Two-sample t-test, with sex and age as covariates,  $p < 0.05$  corrected for Family-wise error (FWE) rate with a cluster size  $\geq 20$  voxels

postcentral gyrus, caudate, putamen, globus pallidus, inferior parietal lobule, claustrum, parahippocampal gyrus, left precentral gyrus, left thalamus, posterior cingulate, and right cingulate gyrus (Table 2).

#### 4. CBF changes measured using ASL after intervention

Hyperperfusion regions were decreased after 12 weeks of intervention in the treatment group only (Figure 4). Hyperperfusion regions before intervention compared with after intervention in the treatment group included the bilateral inferior frontal gyrus, thalamus, precuneus, posterior cingulate, parahippocampal gyrus, left precentral

gyrus, right cingulate gyrus, right caudate, right globus pallidus, and left putamen (Table 3). In contrast, the control group exhibited no significant changes in the hyperperfusion regions after intervention.

#### Adverse events

Patients were encouraged to report all adverse events. During the study period, however, no serious adverse events were reported.

#### Discussion

To explore the therapeutic mechanism of



**Table 2.** Hyperperfusion Regions in the Patients Group Compared with the Healthy Group

Cluster size	Side	Cluster location	Talairach coordinate			Z -score
			X	Y	Z	
2346 (Cluster 1)	L	Insula	-33.62	-12.31	16.96	5.7
	L	Insula	-37.38	-26.44	17.36	5.4
	L	Clastrum	-28.82	13.6	11.38	5.34
4671	L	Sub-Gyral	-14.36	24.71	41.51	5.7
	R	Cingulate Gyrus	6.65	-40.46	43.8	5.65
	R	Postcentral Gyrus	33.59	-22.46	41.45	5.52
1647	L	Precentral Gyrus	-44.93	-0.02	35.95	5.69
	L	Precentral Gyrus	-45.98	-17.39	40.59	5.56
	L	Precentral Gyrus	-42.24	-6.15	40.82	5.37
513	R	Inferior Parietal Lobule	42.83	-30.9	40.81	5.48
	R	Superior Parietal Lobule	31.61	-51.77	43.15	5.13
	R	Inferior Parietal Lobule	42.74	-42.51	44.21	5.04
384 (Cluster 2)	R	Medial Globus Pallidus	14.79	0.54	-0.83	5.44
	R	Putamen	21.13	3.19	10.34	5.19
	R	Hypothalamus	6.47	-2.04	-3.01	4.88
647	L	Posterior Cingulate	-11.43	-50.94	7.37	5.41
	L	Hippocampus	-26.14	-36.45	3.98	5.26
	L	Parahippocampal Gyrus	-16.88	-39.21	2.98	5.23
1736	R	Clastrum	31.15	-15.44	17.76	5.35
	R	Putamen	25.73	5.69	13.36	5.12
	R	Insula	40.35	-24.13	19.79	4.92
137	L	Inferior Parietal Lobule	-47.91	-33.48	41.73	5.27
	L	Postcentral Gyrus	-50.62	-22.03	40.07	5.2
694 (Cluster 3)	R	Caudate Head	1.83	15.25	3.05	5.23
	L	Putamen	-23.31	-0.4	10.15	5.03
	L	Lateral Globus Pallidus	-14.84	1.54	-0.33	4.91
301	L	Inferior Parietal Lobule	-47.97	-51.36	41.84	5.12
	L	Inferior Parietal Lobule	-46.08	-42.81	40.88	4.99
21	R	Middle Frontal Gyrus	36.42	-9.35	41.84	5.09
119	L	Precuneus	-15.36	-59.94	22.66	5.07
197	L	Superior Temporal Gyrus	-44.93	-52.16	21.1	5.05
24	L	Precentral Gyrus	-40.42	-13.69	41.03	5.01
83	L	Insula	-30.47	24.24	-1.15	4.94
494	L	Posterior Cingulate	-9.81	-55.4	24.09	4.92
	L	Posterior Cingulate	-6.01	-43.72	19.85	4.72
	L	Posterior Cingulate	-8.77	-51.83	16.34	4.7
65	R	Clastrum	26.88	25.63	1.75	4.74
292	R	Parahippocampal Gyrus	18.21	-48.13	6.33	4.73
	R	Parahippocampal Gyrus	12.7	-36.83	6.41	4.61
49	R	Inferior Parietal Lobule	41.79	-51.82	43.32	4.69
36	L	Caudate Tail	-17.95	-23.83	18.83	4.57
	L	Thalamus (Ventral Lateral Nucleus)	-14.2	-15.2	17.01	4.42
23	R	Caudate Body	17.36	4.54	15.81	4.54
	R	Caudate Body	17.3	-3.26	18.67	4.4
49	L	Insula	-50.44	-37.14	21.53	4.4
37	R	Anterior Cingulate	7.42	45.61	9.63	4.32

Two-sample t-test, with sex and age as covariates,  $p < 0.05$  corrected for Family-wise error (FWE) rate with a cluster size  $\geq 20$  voxels  
L: Left, R: Right

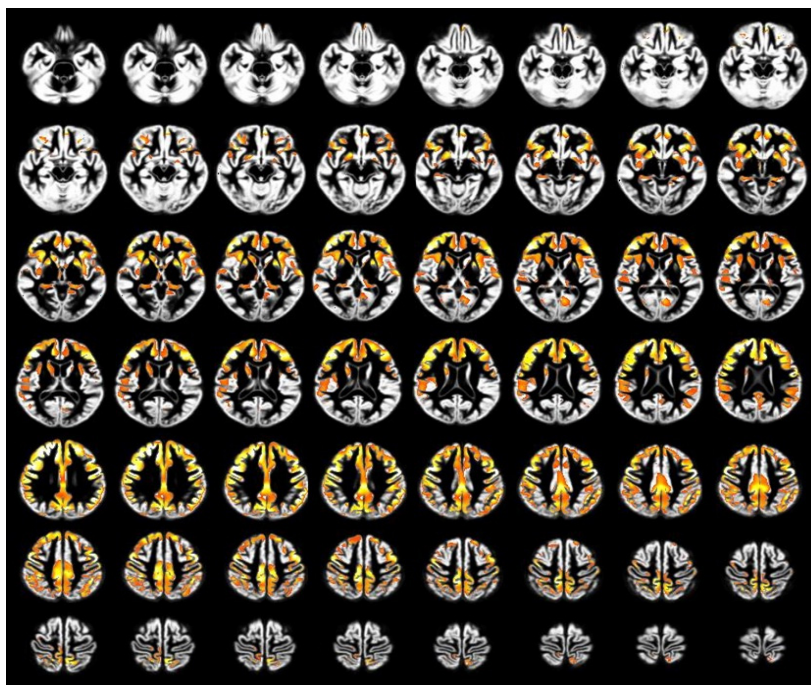


**Fig. 4.** Overlay of results of voxel-wise comparison before and after acupuncture and bee venom acupuncture in the treatment group

Overlaid images show hyperperfusion regions (red color) before treatment compared with after treatment in the treatment group. Paired t-test,  $p < 0.001$  corrected for false discovery rate (FDR) with a cluster size  $\geq 20$  voxels.

acupuncture and BVA in patients with PD, we compared changes in striatal DAT binding and CBF between the acupuncture and BVA treatment group and a sham acupuncture group using PET and ASL.

In the PET results, the striatal DAT binding ratio was increased in both groups after 12 weeks' intervention and the change was larger in the treatment group. The pathophysiological mechanism of PD is known to be the loss of dopaminergic neurons in the substantia nigra pars compacta, most prominently in the striatum. Significant reduction of 18-F DOPA striatal uptake and the correlation with clinical severity in PD has been confirmed in previous studies.<sup>17,23)</sup>

The results of our study suggest that acupuncture and BVA treatment may lead to an increase in DAT binding, which may be a possible therapeutic mechanism of acupuncture and BVA for PD. This is consistent with previous studies that have reported that acupuncture may improve clinical symptoms through alteration of dopamine levels.<sup>7,24,25)</sup> Kim et al.<sup>7)</sup> found that acupuncture treatment at GB34 in MPTP-intoxicated mice increased dopamine availability, likely through enhanced dopamine release, which may result in the normalization of postsynaptic abnormalities. Otherwise, results from the sham control group could be explained by placebo effect, which has been known to influence the degree of striatal

dopamine release in patients with PD.<sup>26)</sup>

In the ASL results, the patient group exhibited hyperperfusion regions compared with the healthy group. The regions included the bilateral insula, postcentral gyrus, caudate, putamen, globus pallidus, inferior parietal lobule, claustrum,

parahippocampal gyrus, left precentral gyrus, left thalamus, posterior cingulate gyrus, and right cingulate gyrus.

After 12 weeks' intervention, ASL-perfusion MR imaging revealed recovered cerebral hyperperfusion in the basal ganglia (caudate, putamen and globus

**Table 3.** Hyperperfusion Regions Before Treatment Compared with After Treatment in the Treatment Group

Cluster size	Side	Cluster location	Talairach coordinate			Z-score
			X	Y	Z	
40886	R	Inferior Frontal Gyrus	37.95	30.81	6.04	5.86
	L	Precentral Gyrus	-51.35	-6.92	29.78	5.58
	R	Cingulate Gyrus	8.86	16.99	33.06	5.49
1099	R	Caudate Head	12.92	8.67	2.61	4.64
	R	Lateral Globus Pallidus	15.66	0.18	2.76	4.51
	R	Thalamus	6.36	-4.69	4.84	4.41
34	L	Precuneus	-23.71	-62.78	23.15	4.33
50	R	Precuneus	14.87	-55	47.96	4.27
89	L	Inferior Frontal Gyrus	-24.83	27.61	-7.04	4.27
192	R	Inferior Frontal Gyrus	29.69	28.58	0.28	4.17
		No Gray Matter found	32.49	36.95	1.12	3.83
		No Gray Matter found	21.39	34.3	-0.22	3.63
47	R	Precuneus	16.71	-60.6	47.46	4.13
416	L	Lingual Gyrus	-9.58	-59.16	4.82	3.99
	L	Parahippocampal Gyrus	-12.24	-46.43	-0.33	3.59
	L	Posterior Cingulate	-5.98	-64.53	11.57	3.47
52	R	Thalamus	3.58	-19.32	0.71	3.96
319	L	Parahippocampal Gyrus	-17.76	-35.22	0.64	3.95
	L	Thalamus (Pulvinar)	-12.23	-29.92	3.94	3.59
	L	Hippocampus	-28.84	-33.12	-1.15	3.56
66	R	Middle Occipital Gyrus	30.85	-77.97	22.64	3.92
273	R	Parahippocampal Gyrus	23.87	-35.52	2.22	3.89
	R	Thalamus (Pulvinar)	20.08	-34.34	9.47	3.53
	R	Parahippocampal Gyrus	23.07	-27.28	-5.12	3.37
118	L	Superior Parietal Lobule	-25.77	-54.27	41.94	3.88
108	R	Insula	43.56	10.14	-3.93	3.84
24	R	Precuneus	36.3	-65.07	34.76	3.78
23	L	Precuneus	-26.69	-47.83	43.44	3.71
95	L	Thalamus (Ventral Anterior Nucleus)	-8.47	-4.78	6.38	3.68
	L	Putamen	-16.85	2.19	12.31	3.6
35	R	Paracentral Lobule	17.74	-35.19	47.19	3.66
26	R	Posterior Cingulate	22.8	-62.12	5.08	3.61

Paired t-test,  $p < 0.001$  corrected for false discovery rate (FDR) with a cluster size  $\geq 20$  voxels.

L: Left, R: Right

pallidus), thalamus, precentral gyrus, and limbic system (parahippocampal gyrus, posterior cingulate and cingulate gyrus) in the treatment group only. In a previous SPECT study investigating localized cerebral perfusion abnormalities in patients with PD, regional CBF in the putamen, globus pallidus, thalamus, brainstem, and the anterior lobe of the cerebellum were significantly higher, and the dorsolateral prefrontal cortex, the insula, and the cingulate gyrus were hypoperfused.<sup>27)</sup> The radiological changes in our study supported that acupuncture and BVA treatment led to recovery of cerebral hyperperfusion in patients with PD, which may explain a possible therapeutic mechanism of acupuncture and BVA.

Although the mechanism of hyperperfusion in the basal ganglia regions in PD is unclear, the loss of dopaminergic neuron innervation may lead to abnormal activities in those regions according to the complicated functional thalamocortex-basal ganglia circuits of PD.<sup>28)</sup> This may imply that neuronal hyperactivity in these regions may result from compensatory hyperperfusion reflected by parkinsonian symptoms. This can be understood as analogous to surgical ablations, such as ventral pallidotomy or ventrolateral thalamotomy, which have been performed to alleviate the clinical symptoms of PD.<sup>29)</sup> Eidelberg et al.<sup>30)</sup> reported that pallidotomy reduced preoperative overaction of the pallidothalamic projection using 18F-fluorodeoxyglucose PET. Therefore, changes in CBF after acupuncture and BVA in those regions in patients with PD have been suggested to be caused by complex feedback mechanisms induced by striatal dopamine deficiency.<sup>31)</sup>

The neurological mechanisms of motor disturbance in patients with PD are believed to be partly related to dysfunction in the basal ganglia motor circuit as well as the primary motor cortex. Repetitive transcranial magnetic stimulation of the primary motor cortex has been used in the treatment of motor symptoms in PD to modulate cortical excitability.<sup>32)</sup> In this study, acupuncture and BVA significantly altered CBF in these regions, and we believe that acupuncture and BVA treatments may be effective for the improvement of motor disturbances in patients with PD.

In the limbic system, previous studies investigating PD have reported diverse CBF results: insula, increase<sup>33,34)</sup> or decrease<sup>27,35)</sup>; parahippocampal gyrus, increase<sup>33,34)</sup> or decrease<sup>27)</sup>; and anterior cingulate, preserved.<sup>36)</sup> The results are inconsistent, and the reason for increased CBF in these regions in our study is unclear, but it may be due to a complex association between the basal ganglia and limbic system in patients with PD. Increased CBF in these regions is considered to be related to pain in patients with PD. The quality and intensity of a painful sensation depend not only on the presence of sensory components but also on affective and cognitive aspects. In an fMRI study exploring the analgesic effects of acupuncture, the cingulate gyrus, insula, and primary somatosensory cortex were modulated by acupuncture.<sup>37)</sup> Most patients with PD commonly experience pain as one of several symptoms, which could be modulated by mediating the dopaminergic and noradrenergic systems, because pain is associated with the activation of the pain matrix (insula, cingulate and prefrontal cortex).<sup>38)</sup>

CBF was significantly altered after 12 weeks of acupuncture and BVA treatments in the treatment group differently from the control group. Generally, acupuncture is known to have a placebo effect; however, the neuroimaging findings from our study indicate that the treatments have a real differentiating neurological effect. PD is a neurological disease in which a prominent placebo effect has been repeatedly reported.<sup>39)</sup> A previous study analyzing 11 medical and surgical treatment trials with 858 patients with PD on placebo reported that the overall placebo response rate was 16% (range: 0 - 55%).<sup>40)</sup> However, the results of our study demonstrated that the mechanisms underlying the effects of the active and the sham treatments were different, and could be evidence that acupuncture has a specific therapeutic effect more than an expected effect.

In previous neuroimaging studies using acupuncture, there were limitations to study design. For example, only one acupuncture point was stimulated in patients with PD. Otherwise, the acupuncture group was compared with a healthy control group, or the acupuncture group was compared with a control group taking antiparkinsonian medication without a sham acupuncture group.<sup>8,9)</sup> However, this study explored the mechanism of acupuncture and BVA, and performed a comparison with a sham control group to overcome these limitations.

In conclusion, we suggest that acupuncture and BVA treatment can alter dopamine availability and normalize hyperperfusion regions specifically related to PD. Normalization of CBF in the basal ganglia and precentral gyrus may lead to improvement in the cardinal symptoms of PD,

and normalization of CBF in the limbic system may lead to improvement in non-motor symptoms including pain. Normalization of CBF in the thalamus could be related to improvements in both motor and non-motor symptoms. In addition, no serious adverse events were observed and no patients dropped out due to side effects in this study. Therefore, acupuncture and BVA treatment are believed to be safe and effective if performed after the bee venom allergy test by a skilled physician.

The present study had some limitations. The sample size was small, and a considerable number of subjects dropped out or were excluded from the analyses because of low-quality images due to reasons such as movement; thus, it was not possible to draw definitive conclusions. Nevertheless, results of this study suggest that the therapeutic mechanism of acupuncture and BVA in PD is different from placebo, as reflected DAT and CBF profiles. Further studies with larger sample sizes are, therefore, warranted.

## Acknowledgements

This work was supported by the Korea Institute of Oriental Medicine [grant number KSN2211010].

## References

1. de Lau, L. M. & Breteler, M. M. (2006). Epidemiology of parkinson's disease. *Lancet Neurol.* 5(6). 525-535. [http://doi.org/10.1016/S1474-4422\(06\)70471-9](http://doi.org/10.1016/S1474-4422(06)70471-9)
2. Yang, J. L., Chen, J. S., Yang, Y. F., Chen, J. C., Lin, C. H., Chang, R. S., et al. (2011).

- Neuroprotection effects of retained acupuncture in neurotoxin-induced parkinson's disease mice. *Brain Behav Immun.* 25(7). 1452-1459. <http://doi.org/10.1016/j.bbi.2011.05.012>
3. Doo, A. R., Kim, S. T., Kim, S. N., Moon, W., Yin, C. S., Chae, Y., et al. (2010). Neuroprotective effects of bee venom pharmaceutical acupuncture in acute 1-methyl-4-phenyl-1,2,3,6-tetrahydropyridine-induced mouse model of parkinson's disease. *Neurol Res.* 32 Suppl 1. 88-91. <http://doi.org/10.1179/016164109X12537002794282>
  4. Ye, M., Chung, H. S., Lee, C., Hyun Song, J., Shim, I., Kim, Y. S., et al. (2016). Bee venom phospholipase a2 ameliorates motor dysfunction and modulates microglia activation in parkinson's disease alpha-synuclein transgenic mice. *Exp Mol Med.* 48(7). e244. <http://doi.org/10.1038/emm.2016.49>
  5. Cho, S. Y., Shim, S. R., Rhee, H. Y., Park, H. J., Jung, W. S., Moon, S. K., et al. (2012). Effectiveness of acupuncture and bee venom acupuncture in idiopathic parkinson's disease. *Parkinsonism Relat Disord.* 18(8). 948-952. <http://doi.org/10.1016/j.parkreldis.2012.04.030>
  6. Doo, K. H., Lee, J. H., Cho, S. Y., Jung, W. S., Moon, S. K., Park, J. M., et al. (2015). A prospective open-label study of combined treatment for idiopathic parkinson's disease using acupuncture and bee venom acupuncture as an adjunctive treatment. *Journal of Alternative and Complementary Medicine.* 21(10). 598-603. <http://doi.org/10.1089/acm.2015.0078>
  7. Kim, S. N., Doo, A. R., Park, J. Y., Bae, H., Chae, Y., Shim, I., et al. (2011). Acupuncture enhances the synaptic dopamine availability to improve motor function in a mouse model of parkinson's disease. *PLoS One.* 6(11). e27566. <http://doi.org/10.1371/journal.pone.0027566>
  8. Yeo, S., Choe, I. H., van den Noort, M., Bosch, P., Jahng, G. H., Rosen, B., et al. (2014). Acupuncture on GB34 activates the precentral gyrus and prefrontal cortex in parkinson's disease. *BMC Complement Altern Med.* 14. 336. <http://doi.org/10.1186/1472-6882-14-336>
  9. Yeo, S., Lim, S., Choe, I. H., Choi, Y. G., Chung, K. C., Jahng, G. H., et al. (2012). Acupuncture stimulation on GB34 activates neural responses associated with parkinson's disease. *CNS Neurosci Ther.* 18(9). 781-790. <http://doi.org/10.1111/j.1755-5949.2012.00363.x>
  10. Loane, C. & Politis, M. (2011). Positron emission tomography neuroimaging in parkinson's disease. *Am J Transl Res.* 3(4). 323-341.
  11. Amorim, B. J. Camargo, E. C. & Etchebehere, E. C. (2007). Regional CBF changes in parkinson's disease: The importance of functional neuroimaging analyses. *Eur J Nucl Med Mol Imaging.* 34(9). 1455-1457. <http://doi.org/10.1007/s00259-007-0411-8>
  12. Tupala, E., Kuikka, J. T., Hall, H., Bergstrom, K., Sarkioja, T., Rasanen, P., et al. (2001). Measurement of the striatal dopamine transporter density and heterogeneity in type 1 alcoholics using human whole hemisphere autoradiography. *Neuroimage.* 14(1). 87-94. <http://doi.org/10.1006/nimg.2001.0793>
  13. Fernandez-Seara, M. A., Aznarez-Sanado, M.,

- Mengual, E., Irigoyen, J., Heukamp, F. & Pastor, M. A. (2011). Effects on resting cerebral blood flow and functional connectivity induced by metoclopramide: A perfusion MRI study in healthy volunteers. *Br J Pharmacol.* 163(8). 1639-1652. <http://doi.org/10.1111/j.1476-5381.2010.01161.x>
14. Detre, J. A. & Wang, J. J. (2002). Technical aspects and utility of fmri using bold and asl. *Clinical Neurophysiology.* 113(5). 621-634. [http://doi.org/10.1016/S1388-2457\(02\)00038-X](http://doi.org/10.1016/S1388-2457(02)00038-X)
15. Hughes, A. J., Daniel, S. E., Kilford, L. & Lees, A. J. (1992). Accuracy of clinical diagnosis of idiopathic parkinson's disease: A clinico-pathological study of 100 cases. *J Neurol Neurosurg Psychiatry.* 55(3). 181-184. <http://doi.org/10.1136/jnnp.55.3.181>
16. Hoehn, M. M. & Yahr, M. D. (1967). Parkinsonism: Onset, progression and mortality. *Neurology.* 17(5). 427-442. <http://doi.org/10.1212/wnl.17.5.427>
17. Jin, S., Oh, M., Oh, S. J., Chung, S. J., Lee, C. S. & Kim, J. S. (2012). Differential diagnosis of parkinsonism using dual-phase F-18 FP-CIT PET imaging. *European Journal of Nuclear Medicine and Molecular Imaging.* 47(1). 44-51. <http://doi.org/10.1007/s13139-012-0182-4>.
18. Edelman, R. R., Siewert, B., Darby, D. G., Thangaraj, V., Nobre, A. C., Mesulam, M. M., et al. (1994). Qualitative mapping of cerebral blood-flow and functional localization with echo-planar MR-imaging and signal targeting with alternating radio-frequency. *Radiology.* 192(2). 513-520. <http://doi.org/10.1148/radiology.192.2.8029425>
19. Golay, X., Petersen, E. T. & Hui, F. (2005). Pulsed star labeling of arterial regions (PULSAR): A robust regional perfusion technique for high field imaging. *Magnetic Resonance in Medicine.* 53(1). 15-21. <http://doi.org/10.1002/mrm.20338>
20. Kim, S. M., Kim, M. J., Rhee, H. Y., Ryu, C. W., Kim, E. J., Petersen, E. T., et al. (2013). Regional cerebral perfusion in patients with alzheimer's disease and mild cognitive impairment: Effect of APOE epsilon4 allele. *Neuroradiology.* 55(1). 25-34. <http://doi.org/10.1007/s00234-012-1077-x>
21. Wang, Z., Aguirre, G. K., Rao, H., Wang, J., Fernandez-Seara, M. A., Childress, A. R., et al. (2008). Empirical optimization of asl data analysis using an asl data processing toolbox: Aslrbx. *Magnetic Resonance Imaging.* 26(2). 261-269. <http://doi.org/10.1016/j.mri.2007.07.003>
22. Ashburner, J. (2007). A fast diffeomorphic image registration algorithm. *Neuroimage.* 38(1). 95-113. <http://doi.org/10.1016/j.neuroimage.2007.07.007>
23. Berti, V., Pupi, A. & Mosconi, L. (2011). PET/CT in diagnosis of movement disorders. *Ann N Y Acad Sci.* 1228(93-108). <http://doi.org/10.1111/j.1749-6632.2011.06025.x>
24. Rui, G., Guangjian, Z., Yong, W., Jie, F., Yanchao, C., Xi, J., et al. (2013). High frequency electro-acupuncture enhances striatum DAT and D1 receptor expression, but decreases D2 receptor level in 6-OHDA lesioned rats. *Behav Brain Res.* 237. 263-269. <http://doi.org/10.1016/j.bbr.2012.09.047>
25. Kim, S. N., Doo, A. R., Park, J. Y., Choo, H. J., Shim, I., Park, J. J., et al. (2014). Combined

- treatment with acupuncture reduces effective dose and alleviates adverse effect of L-dopa by normalizing parkinson's disease-induced neurochemical imbalance. *Brain Res.* 1544. 33-44. <http://doi.org/10.1016/j.brainres.2013.11.028>
26. Lidstone, S. C., Schulzer, M., Dinelle, K., Mak, E., Sossi, V., Ruth, T. J., et al. (2010). Effects of expectation on placebo-induced dopamine release in parkinson disease. *Arch Gen Psychiatry.* 67(8). 857-865. <http://doi.org/10.1001/archgenpsychiatry.2010.88>
  27. Hsu, J. L., Jung, T. P., Hsu, C. Y., Hsu, W. C., Chen, Y. K., Duann, J. R., et al. (2007). Regional CBF changes in parkinson's disease: A correlation with motor dysfunction. *European Journal of Nuclear Medicine and Molecular Imaging.* 34(9). 1458-1466. <http://doi.org/10.1007/s00259-006-0360-7>
  28. Alexander, G. E., Crutcher, M. D. & DeLong, M. R. (1990). Basal ganglia-thalamocortical circuits: Parallel substrates for motor, oculomotor, "prefrontal" and "limbic" functions. *Prog Brain Res.* 85. 119-146.
  29. Dogali, M., Fazzini, E., Kolodny, E., Eidelberg, D., Sterio, D., Devinsky, O., et al. (1995). Stereotactic ventral pallidotomy for parkinson's disease. *Neurology.* 45(4). 753-761. <http://doi.org/10.1212/wnl.45.4.753>
  30. Eidelberg, D., Moeller, J. R., Ishikawa, T., Dhawan, V., Spetsieris, P., Silbersweig, D., et al. (1996). Regional metabolic correlates of surgical outcome following unilateral pallidotomy for parkinson's disease. *Annals of Neurology.* 39(4). 450-459. <http://doi.org/10.1002/ana.410390407>
  31. Antonini, A., Vontobel, P., Psylla, M., Gunther, I., Maguire, P. R., Missimer, J., et al. (1995). Complementary positron emission tomographic studies of the striatal dopaminergic system in parkinson's disease. *Arch Neurol.* 52(12). 1183-1190. <http://doi.org/10.1001/archneur.1995.00540360061017>
  32. Zanjani, A., Zakzanis, K. K., Daskalakis, Z. J. & Chen, R. (2015). Repetitive transcranial magnetic stimulation of the primary motor cortex in the treatment of motor signs in parkinson's disease: A quantitative review of the literature. *Mov Disord.* 30(6). 750-758. <http://doi.org/10.1002/mds.26206>
  33. Fernandez-Seara, M. A., Mengual, E., Vidorreta, M., Aznarez-Sanado, M., Loayza, F. R., Villagra, F., et al. (2012). Cortical hypoperfusion in parkinson's disease assessed using arterial spin labeled perfusion MRI. *Neuroimage.* 59(3). 2743-2750. <http://doi.org/10.1016/j.neuroimage.2011.10.033>
  34. Imon, Y., Matsuda, H., Ogawa, M., Kogure, D. & Sunohara, N. (1999). Spect image analysis using statistical parametric mapping in patients with Parkinson's disease. *Journal of Nuclear Medicine.* 40(10). 1583-1589.
  35. Kikuchi, A., Takeda, A., Kimpara, T., Nakagawa, M., Kawashima, R., Sugiura, M., et al. (2001). Hypoperfusion in the supplementary motor area, dorsolateral prefrontal cortex and insular cortex in Parkinson's disease. *Journal of the Neurological Sciences.* 193(1). 29-36. [http://doi.org/10.1016/S0022-510x\(01\)00641-4](http://doi.org/10.1016/S0022-510x(01)00641-4)
  36. Melzer, T. R., Watts, R., MacAskill, M. R., Pearson, J. F., Rueger, S., Pitcher, T. L., et al. (2011). Arterial spin labelling reveals an abnormal cerebral perfusion pattern in



- parkinson's disease. *Brain*. 134. 845-855. <http://doi.org/10.1093/brain/awq377>
37. Theysohn, N., Choi, K. E., Gizewski, E. R., Wen, M., Rampp, T., Gasser, T., et al. (2014). Acupuncture-related modulation of pain-associated brain networks during electrical pain stimulation: A functional magnetic resonance imaging study. *Journal of Alternative and Complementary Medicine*. 20(12). 893-900. <http://doi.org/10.1089/acm.2014.0105>
38. Ballanger, B., Poisson, A., Broussolle, E. & Thobois, S. (2012). Functional imaging of non-motor signs in parkinson's disease. *Journal of the Neurological Sciences*. 315(1-2). 9-14. <http://doi.org/10.1016/j.jns.2011.11.008>
39. de la Fuente-Fernandez, R., Schulzer, M. & Stoessel, A. J. (2002). The placebo effect in neurological disorders. *Lancet Neurology*. 1(2). 85-91. [http://doi.org/10.1016/S1474-4422\(02\)00038-8](http://doi.org/10.1016/S1474-4422(02)00038-8)
40. Goetz, C. G., Wu, J., McDermott, M. P., Adler, C. H., Fahn, S., Freed, C. R., et al. (2008). Placebo response in parkinson's disease: Comparisons among 11 trials covering medical and surgical interventions. *Movement Disorders*. 23(5). 690-699. <http://doi.org/10.1002/mds.21894>

## ORCID

Young-Eun Lee	<a href="https://orcid.org/0009-0004-0606-7713">https://orcid.org/0009-0004-0606-7713</a>
Seung-Yeon Cho	<a href="https://orcid.org/0000-0003-3149-9759">https://orcid.org/0000-0003-3149-9759</a>
Han-Gyul Lee	<a href="https://orcid.org/0000-0001-7355-5638">https://orcid.org/0000-0001-7355-5638</a>
Seungwon Kwon	<a href="https://orcid.org/0000-0002-1857-3515">https://orcid.org/0000-0002-1857-3515</a>
Woo-Sang Jung	<a href="https://orcid.org/0000-0001-7355-7684">https://orcid.org/0000-0001-7355-7684</a>
Sang-Kwan Moon	<a href="https://orcid.org/0000-0003-0497-3080">https://orcid.org/0000-0003-0497-3080</a>
Jung-Mi Park	<a href="https://orcid.org/0000-0002-0851-4431">https://orcid.org/0000-0002-0851-4431</a>
Chang-Nam Ko	<a href="https://orcid.org/0000-0002-4749-7961">https://orcid.org/0000-0002-4749-7961</a>
Seong-Uk Park	<a href="https://orcid.org/0000-0002-4617-2719">https://orcid.org/0000-0002-4617-2719</a>